

Classicality of Spin Coherent States via Entanglement and Distinguishability

D. Markham and V. Vedral

Optics Section, Blackett Laboratory, Imperial College, London SW7 2BW, United Kingdom.

(Dated: May 21, 2019)

We investigate the classical nature of the spin coherent states. In addition to being minimum uncertainty states, as the size of the spin, S , increases, the classical nature is seen to increase in two respects: in their resistance to entanglement generation (when passed through a beam splitter) and in the distinguishability of the states. In the infinite S limit the spin coherent state is a subclass of the optical coherent states (namely the subclass of orthogonal optical coherent states). These states generate no entanglement and are obviously completely distinguishable. The decline of the generated entanglement, and in this sense increase in classicality with S , is very slow and dependent on the amplitude z of the state. Surprisingly we find that for $|z| > 1$ there is an initial increase in entanglement followed by an extremely gradual decline to zero. The distinguishability, on the other hand, quickly becomes classical for all z . We illustrate the distinguishability of spin coherent states in a novel manner using the representation of Majorana.

INTRODUCTION

The transition from the quantum to the classical world is not fully understood at present. Although classical physics is believed to be a limiting case of quantum mechanics, it is frequently unclear which limit should be taken and how this is to be achieved. We can, for example, try to think of how the laws of physics come to appear as the classical laws if we start from the Schrödinger equation as in [1]. Alternatively, we might think about how physical objects themselves come to appear classical, when they are so manifestly quantum at the most basic level that we can test in our most accurate experiments. In this case, initial quantum states describing objects would somehow have to make a transition to become classical. Quantum physics has been considered to approach the classical in many different ways and we name several of them: 1) as \hbar goes to zero, the variance (or uncertainty) of a measure goes to zero and we can separate all states perfectly (this is known as Bohr's correspondence principle); also, the classical Hamilton-Jacobi dynamics can be "derived" from the Schrödinger equation in this limit; 2) positivity of the Wigner or P-function is often taken to imply classicality, since they then can be thought of as representing real probability functions as in classical statistical mechanics; 3) the entanglement present in a collection of states is clearly an indication of nonclassicality and a lack of it can be construed as signature of classicality (various decoherence pictures, on the other hand, use the entanglement with the environment as a signature of classicality; in this case the global presence of entanglement leads to classicality); 4) minimisation of uncertainty for two non commuting variables; 5) distinguishability of states (classical states are always fully distinguishable at least in principle). Although each of these criteria is adequate in its own domain, it needs to be stressed that they are by no means equivalent. In fact, they frequently contradict each other. A well known example of this is that a state of two light modes can be entangled and still have an overall positive Wigner function, as well as vice versa. It is, therefore, very important to investigate the relationship between these various approaches in order to gain a deeper understanding of the transition between the quantum and the classical. In this paper we investigate classical features of general spin coherent states as they allow us to trace the whole spectrum of quantum states, starting from what we call here the "least" classical states (i.e. spin half) up to the "most" classical states (i.e. optical coherent states) by changing the magnitude of the spin, S , from $1/2$ to ∞ .

One of the first states defined specifically with classicality in mind is the optical coherent states or Glauber states [2]. These states can be created from classical electromagnetic fields and can be seen to be classical in three of the respects mentioned above. Firstly, an optical coherent state is (by definition) a state of minimum uncertainty. Then, and speaking somewhat loosely, as their amplitude tends to infinity (meaning that the number of photons becomes arbitrarily large), optical coherent states become orthogonal and therefore distinguishable. In this way, we can think of a laser beam of many photons as completely distinguishable from another such laser beam. The third way is their action through a beam splitter. It has been proven that the optical coherent state is the only pure state that when passed through one arm of a beam splitter (with the other arm being a vacuum) returns a product state, which is a state with zero entanglement [3].

The Glauber states can then be generalised in different ways to a wider set of states, including minimum-uncertainty-defined states and group-defined states (see [4] and [5] for good reviews). One such generalisation is the spin coherent state, introduced in [6] and [7], which has been compared to the optical state and many parallels have been drawn. For example, it too is a state of minimum uncertainty and can be produced by classical fields. In this paper, we extend this comparison and analysis of the classicality of the spin coherent state to looking at entanglement created

through a beam splitter and their distinguishability using the Helstrom measurement strategy, across the range in S from $S = 1/2 \rightarrow \infty$.

In particular, in the first section we investigate the entanglement of the state generated by passing it through one arm of a beam splitter while the other arm is left in the empty vacuum state. It is known that, in the infinite spin limit, spin coherent states are a subclass of the optical coherent states ([7],[6]). Thus in the infinite limit the generated entanglement goes to zero. We present a different proof in terms of the states in the first quantisation. Our method has the advantage that it easily follows that there are infinitely many other classical states of the same dimensionality as spin coherent state with the same property that they asymptotically approach the Glauber states. We find that the reluctance to entanglement is very slow to increase with S and is only near zero for very high S . In addition the entanglement creation is dependant on z and for $|z| > 1$ we see a surprising rise in entanglement - hence decline in classicality. This is explained and parallels drawn to another similar case noted by Arnesen et al [8]. The validity of this as a measure of classicality is then discussed.

In the second section we investigate the change in distinguishability of the state with the spin S in terms of the probability of error for a Helstrom optimal measurement. We find that the probability of error decreases rapidly with S , hence the distinguishability and classicality in this sense increases rapidly to a maximum level. This transition is smooth and quick from the least classical spin $1/2$ state to the most classical limit $S \rightarrow \infty$. We then go on to look at the Helstrom best measurement strategy with the novel Majorana representation. For an n dimensional state system, the Majorana representation defines the state (up to a global phase) by $n - 1$ points on the surface of a Riemann sphere. Geometric interpretation of physical systems is often very helpful in gaining further intuition. For example the Bloch sphere can be used to see intuitively the way optimal fidelity is achieved in cloning [9]. The Majorana representation shows well the changes in the measures affected by changing S for the spin coherent states in a simple geometry.

Conclusions are finally drawn and comments made about the nature and validity of the results found. We compare the two methods of accessing classicality with each other and other existing and proposed methods. We also suggest a number of further investigations that can be carried out along the lines of the present work.

ACTION THROUGH A BEAM SPLITTER

In optics the action of a beam splitter is described as a particular kind of a mixer of two beams of light or, more mathematically, two modes of the quantised electromagnetic field. A 50/50 beam splitter takes an input state comprised of a general n photon Fock state in one mode and a ground (vacuum) Fock state in the other, $|n, 0\rangle$, to a superposition of binomially populated modes:

$$U_{bs}|n, 0\rangle = \sum_{p=0}^n \binom{n}{p}^{1/2} 2^{-n/2} |p, n-p\rangle. \quad (1)$$

In general these resultant states will be entangled, indeed, for any input made up of a finite superposition of Fock states the entanglement cannot be zero (except, of course, in the case of the trivial ground state). This can easily be proved by tracing one of the output modes and checking that the resulting state (of the other mode) is strictly mixed, i.e. its trace is less than one. Since we will only deal with overall pure states in our paper, this method for quantifying entanglement will be adequate in general and we will use it later on in this section. We choose a 50/50 beam splitter it is in some sense most efficient at generating entanglement providing we have the above specific scenario of one input arm in the vacuum state (e.g. the input state $|1, 0\rangle$ would be transformed to a maximally entangled Bell state).

An optical coherent state is defined as $|\alpha\rangle = \exp(-\frac{1}{2}|\alpha|^2) \sum_{n=0}^{\infty} \frac{\alpha^n}{(n!)^{1/2}} |n\rangle$ [10]. When this enters one mode and a ground state the other, the output state is $|\psi_{out}\rangle = U_{bs}|\alpha, 0\rangle = \exp(-\frac{1}{2}|\alpha|^2) \sum_{n=0}^{\infty} \sum_{p=0}^n \binom{n}{p}^{1/2} \frac{\alpha^n}{2^{n/2}(n!)^{1/2}} |p, n-p\rangle$ which reduces to the product state $|\psi_{out}\rangle = \exp(-\frac{1}{2}|\alpha|^2) \sum_{p=0}^{\infty} \frac{\alpha^p}{2^{p/2}(p!)^{1/2}} |p\rangle \otimes \sum_{n-p=0}^{\infty} \frac{\alpha^{n-p}}{2^{(n-p)/2}(n-p!)^{1/2}} |n-p\rangle = |\alpha/\sqrt{2}\rangle |\alpha/\sqrt{2}\rangle$. It has been proven that the optical coherent state is the only state that when passed through one arm of a beam splitter returns a product state, with no entanglement [3]. Therefore it is the only classical state within this framework.

Although the beam splitter needs to be defined in a more general way (by giving the transformation of the general basis state $|n, m\rangle$, or, equally well, by defining the action of annihilation and creation operators on the different modes as in for example [11]), it will for us be sufficient to use equation (1) as a specialised definition on the state $|n, 0\rangle$. We now ask what action such a beam splitter makes on a spin coherent state and to what extent the output state depends on the magnitude of the spin.

A spin coherent state $|z\rangle$ is defined here to be the minimum uncertainty, complex rotation of the ground state, parameterised by a complex amplitude z [7], [4], [6]. In terms of the spin step up operator \hat{S}_+ acting on the ground state, we have that

$$|z\rangle = \frac{1}{(1 + |z|^2)^S} \exp^{\bar{z}\hat{S}_+/\hbar} |0\rangle. \quad (2)$$

Expanding the exponential we get

$$|z\rangle = \frac{1}{(1 + |z|^2)^S} \sum_n \binom{2S}{n}^{1/2} \bar{z}^n |n\rangle. \quad (3)$$

The summation only goes up to $2S$ since it is unreasonable to have \hat{S}_+ acting on n greater than $n = 2S$, i.e. we set, for $m > 2S$, $\hat{S}_+|m\rangle = 0$. The uncertainty relation for the spin operators, defined with algebra $[\hat{S}_i, \hat{S}_j] = i\hbar\hat{S}_k$, is given by

$$\langle \hat{S}_i^2 \rangle \langle \hat{S}_j^2 \rangle \geq \frac{1}{4} \hbar^2 \langle \hat{S}_k \rangle^2. \quad (4)$$

This equality holds for the state $|z\rangle$, hence the spin coherent state is also a minimum uncertainty state. Thus in the sense of uncertainty of the above defined non-commuting observables, the spin coherent state is as classical as possible for all S and can be said to have classicality of uncertainty.

In [7] and [6] it is shown by means of the second quantisation, in terms of the operators generating the state, that the limit takes the spin coherent state to the optical coherent state. We now look at this limit purely in terms of the first quantisation and we begin by noticing that, with the appropriate amplitude relationship, as S goes to infinity the spin coherent states represent a subclass of optical coherent states, namely those that are orthogonal. Setting $\alpha = \sqrt{2S}\bar{z}$ provides a suitable substitution. To prove the equivalence it is enough to show that the overlap between the optical coherent state $|\alpha\rangle$ and the spin coherent state $|z'\rangle$ with this substitution goes to 1 in the infinite S limit. That is we wish to prove

$$\begin{aligned} \lim_{S \rightarrow \infty} \langle \alpha | z' \rangle &= \lim_{S \rightarrow \infty} \left\{ \exp\left(-\frac{1}{2}|\alpha|^2\right) \frac{1}{(1 + \frac{|\alpha|^2}{2S})^S} \sum_{n=0}^{2S} \left(\frac{2S!}{(2S-n)!(2S)^n}\right)^{1/2} \frac{|\alpha|^{2n}}{n!} \right\} \\ &= 1. \end{aligned} \quad (5)$$

We can see that the normalisation term outside the sum clearly goes to the exponential in the limit. We also see that each term in the sum goes to $\frac{|\alpha|^{2n}}{n!}$ in the limit. The limit of the sum then gives an inverse exponential. Since both terms converge in the same limit, the product of these terms converges to the product of the convergences and so gives us a product of two exponentials in the limit which cancel to give one. A detailed proof can be found in the Appendix (the orthogonality of these states is discussed later). This result shows that in the infinite S limit, the spin coherent states do not entangle when put through one arm of a beam splitter (since they are in fact optical coherent states). We also see that infinitely many other states can also have this property of asymptotically converging to the optical coherent states (as shown in the Appendix). Therefore, on this ground alone, spin coherent states are no more classical than infinitely many other possible sets of states.

We now wish to see exactly how the entanglement reaches this zero limit. More precisely, we would like to determine if entanglement falls quickly off with increasing spin, such that any reasonably large spin system effectively returns a product state or if indeed the drop off is monotonic at all. The action of a beam splitter on an input state comprising of a spin coherent state in one mode/arm and the vacuum state in the other gives

$$U_{bs}|z, 0\rangle = \frac{1}{(1 + |z|^2)^S} \sum_{n=0}^{2S} \sum_{p=0}^n \binom{2S}{n}^{1/2} \binom{n}{p}^{1/2} 2^{-n/2} \bar{z}^n |p, n-p\rangle. \quad (6)$$

To quantify this non classical nature, we use the linear entropy (see for example [12]) as our measure for entanglement, defined for a bipartite state ρ_{AB} as

$$E = 1 - Tr(\rho_A^2). \quad (7)$$

where $\rho_A = Tr_B(\rho_{AB})$ is the reduced density matrix of system A . The choice of linear entropy rather than the normally used Von Neumann entropy [13] is purely for computational ease and is perfectly valid (as is almost any other function of Schmidt coefficients [14]). It too gives a measure of how mixed the local state ρ_A is, which is essentially a measure of how much information is shared across the state, or how entangled the state is (more precisely the linear entropy of entanglement is a lower bound to the Von Neumann entropy of entanglement).

The entanglement of the two ‘‘beams’’ is then given by:

$$E = 1 - \frac{1}{(1 + |z|^2)^{4S}} \sum_{p,p'=0}^{2S} \left(\sum_{m,}^{\min(2S-p, 2S-p')} \frac{2^{-m} |z|^{2m}}{m!} \left(\frac{1}{(2S - m - p)!(2S - m - p')!} \right)^{1/2} \right)^2 \times \frac{2^{-(p+p')} |z|^{2(p+p')}}{p!p'!} \quad (8)$$

This is not a closed form solution as it were, so we need to investigate it numerically for qualitative results.

Plotting this linear entanglement against S for a fixed $|z|^2 = 1$ (figure 1), we see a quick initial decline followed by a very gradual decrease after around $S = 40$, such that it hardly appears to decrease - though we know that the decrease does happen, and in the limit goes to zero, because the spin coherent state becomes the optical coherent state. This is not the pattern we see for other z , for example, when $|z|^2 = 10$, we see an initial increase, followed by a very gradual decrease (figure 2). This initial increase remains for any $|z|^2$ higher than around 1 and the decrease is slower for higher $|z|$, as can be seen in figure 3, where we plot entanglement against $|z|^2$ and S . We also see that the higher the $|z|$, the higher the generated entanglement for any S . This result is counter to what we might hope as we increase S . The classicality of spin coherent states, in the sense of this entanglement generation, is very dependent on the amplitude of the coherent state and the classical nature is only really seen in the infinite limit. The initial increase of entanglement with $|z| > 1$ is surprising precisely because with increasing S we expect the classical nature of this state to increase, but, instead, its entanglement generation capacity through a beam splitter increases. This initial increase can be put down to the addition of the highly entangled states to the superposition (equation (6)), which is then countered as more less entangled states are added. This does not happen for z less than around unity because the coefficients for the higher entangled states in the superposition decrease for higher orders.

We note that a similar phenomenon was seen in [8], where the authors studied the entanglement between two spin 1/2 particles in a mixed thermal state with an external magnetic field according to the antiferromagnetic Heisenberg model. For some field strengths, as the temperature of the chain increased, there was an initial increase in entanglement, though in the large limit the entanglement went down to zero, as we would expect for such a mixed system. The increase can be put down to the inclusion of highly entangled states in the mixture, which then becomes countered as the mixture dilutes as it extends to more states. The difference being that in our case the increase came from the addition of states to a pure superposition and in theirs they are added in the mixture.

Given this, we may then ask if we can think of a state that is more classical in this sense, namely that generates less entanglement and decreases more rapidly with dimension of the Hilbert space? This is a complicated problem, since the only finite state to give non entangled states through a beam splitter is the ground or vacuum state. The spin coherent states can be arbitrarily close to this zero entanglement, but that is simply because they are arbitrarily close to the ground state in some sense. We then ask how valid this measure of classicality is. For example, we could think of other unitary transformations that would create more entanglement with the input states here, indeed the amount of entanglement generated for a given transformation is dependent on the input state. We can talk of the entangling capacity of a unitary transformation [15], which is a maximum taken over all input states, but again, to define a class of minimum entangling states for one unitary transformation does not mean it is the class of minimum entangling states for a different unitary transformation. The beam splitter transformation is a very specific example, which is important in showing the classicality of the optical coherent state, but there is no reason to choose this one over other transformations as a general measure. As such we can claim that this is not an ideal measure, indeed as a concept, the resistance to entanglement generation of a state is not well defined.

It is still interesting in its own right, however, to see how this class of states is affected when passed through one arm of a beam splitter, since beam splitters are among the simplest devices implementable by experiment and have many applications, including entanglement generation itself (for example [16]); so it is valuable to understand them better in any scenario, especially one involving entanglement generation, as is this one. Indeed as an entanglement generator for the specific scenario of a coherent state, $|z\rangle$, entering one arm and a vacuum state, $|0\rangle$, the other, we can point out some more interesting results about the beam splitter. We can see that the higher the amplitude of $|z\rangle$, the higher the generated entanglement for any S . Also, for a given S there is an amplitude z that gives a maximal entanglement possible and this increases with S .

It is also informative to consider the physical notion of a beam splitter in the sense described above. In the case of the optical state, when we use the term “beam” we usually mean literally beam, or mode of light, that is defined by the path it takes. The action of the beam splitter is then to split the incoming photons of one mode (or path) into two, so the photons leave in a superposition of both paths. This can be written in terms of the creation and annihilation operators, whence the beam splitter annihilates photons from the input path and creates photons in both output paths. With spin coherent states this is not so clear. The analogous operators to the annihilation and creation operators are the step up and down operators. The analogy of creating a photon in a beam would be to add a unit of spin to the system (though the analogy is not exact because of different commutation relations which changes the beam splitter transformation, but broadly speaking it still accomplishes the same). With this in mind one possible interpretation of a spin S system in terms of a symmetric superposition of $2S$ spin $1/2$ systems. Hence one can think of beam of spin $1/2$ particles being split into two paths, where the increase of one unit of spin is equivalent to the addition of a spin $1/2$ particle. In this way the addition of more particles increases the total spin and so makes the system more “classical”, as is the case for optical states, where the more photons there are (the higher the amplitude) the more classical the system can be said to be in terms of distinguishability and entanglement (the states out of a beam splitter are only the same as the input in the infinite limit of α). This view of a spin S system has a natural link to the Majorana representation to be discussed later, since it can be seen as an illustration of these particles.

COHERENT STATE DISCRIMINATION

One of the fundamental principles of quantum mechanics is the uncertainty relation between incompatible observables which, in turn, prohibits us from distinguishing two nonorthogonal states perfectly with one measurement. This strongly contrasts with the classical world where, at least in principle, all states can be distinguished perfectly. We can, however, optimise our measurement strategy in quantum mechanics to give us the most reliable answer possible. One such strategy is that given by Helstrom [17] (see also [18] for a very readable account) where a measurement is made to give two outcomes, one corresponding to each of the states, with a minimal probability of error. We briefly state some of those results before applying them to analysing spin coherent states.

Suppose that we are given a system we know to be in one of two states, ρ_A or ρ_B with probabilities p_A and p_B respectively. When trying to ascertain which of two nonorthogonal states we have, we construct a two outcome generalised measurement, or positive operator-valued measure (POVM), made up of \hat{E}_A and $\hat{E}_B = \mathbf{1} - \hat{E}_A$ and associate the states with the corresponding results. The probability of being incorrect in our association is given by

$$P_e = p_A \text{tr}(\rho_A \hat{E}_B) + p_B \text{tr}(\rho_B \hat{E}_A). \quad (9)$$

For us it is important that in the case of pure states $|A\rangle$ and $|B\rangle$ this POVM becomes a projection measurement with the probability of error given by

$$P_e = p_A \text{tr}(\hat{E}_B |A\rangle\langle A|) + p_B \text{tr}(\hat{E}_A |B\rangle\langle B|). \quad (10)$$

Optimisation of this expression comes through our choice in the projection measurements. Heuristically we wish to choose the projection spaces of \hat{E}_A and \hat{E}_B such that $|A\rangle$ and \hat{E}_B are as close to orthogonal as possible, similarly for $|B\rangle$. This must be balanced against the apriori probabilities to give the minimum probability of error. Helstrom showed that the minimum probability of error in discriminating two pure states is given by

$$P_e = \frac{1}{2} \left(1 - \sqrt{1 - 4p_A p_B |\langle A|B\rangle|^2} \right). \quad (11)$$

We now wish to look at this as our measure of distinguishability (or indistinguishability) for spin coherent states. We begin again by looking at the infinite limit. As mentioned earlier, as $S \rightarrow \infty$ all spin coherent states become orthogonal, that is the overlap tends to zero. This can be easily seen. Two spin coherent states, $|\alpha\rangle$ and $|\beta\rangle$ have overlap $|\langle \alpha|\beta\rangle| = \frac{|(1+\alpha\bar{\beta})^{2S}|}{|(1+|\alpha|^2)^S(1+|\beta|^2)^S|}$. Since $|(1+\alpha\beta^*)^2| \leq |(1+|\alpha|^2)(1+|\beta|^2)|$, the limit in S gives $\lim_{S \rightarrow \infty} |\langle \alpha|\beta\rangle| = 0$ except when the equality is reached, i.e. equal α and β , which, for all S , has $|\langle \alpha|\alpha\rangle| = 1$. Thus in the limit of large S all spin coherent states are orthonormal to each other and hence are entirely distinguishable from one another (as can be seen in equation (11) as P_e vanishes).

We can then look at how this distinguishability changes with S . When attempting to distinguish two spin coherent states $|\alpha\rangle$ and $|\beta\rangle$ we get

$$P_e = \frac{1}{2} \left(1 - \sqrt{1 - 4p_A p_B \left| \frac{(1 + \alpha\bar{\beta})^{2S}}{(1 + |\alpha|^2)^S (1 + |\beta|^2)^S} \right|^2} \right). \quad (12)$$

In figure 4 we plot the probability of error against S for $\alpha = 0, \beta = 1$ and $p_A = p_B = 1/2$ (which, since $p_A + p_B = 1$, clearly gives the largest probability of error), we see a very quick decrease in P_e such that it is negligible by around $S = 4$. This trend of rapid decrease remains for all α and β where they are significantly different. To look at this it is sufficient to consider states with $\alpha = 0$ and $\beta \in R$ since P_e depends on the modulus of the overlap. In figure 5, we plot P_e against S and β (real), again for $p_A = p_B = 1/2$ since this is the maximum error and will show the trends best. We see that the smallest S gives the highest probability of error and the decrease with S is monotonic for all β (real) (as can be verified easily by looking at equation (12)). We also see that, for all S , as β gets larger the probability of error decreases and for $S > 1$ goes to near zero. As β approaches $\alpha = 0$, P_e approaches half, that of a random guess, no matter the S , which we would expect since two equal states can never be told apart. In the interesting region, as β increases away from α , the rapid decrease of P_e with S appears very quickly, so that, for all but near zero difference in α and β , the classicality in the sense of distinguishability emerges very quickly. Plotting the same graph with different p_A, p_B will give smaller values of P_e and not change the overall trends. We can say that the spin coherent states have a smooth and quick transition of classicality of distinguishability, from the $S = 1/2$ least classical state, to the infinite limit, which is completely distinguishable thus most classical.

It is interesting to compare this to the natural curvature of the space of the set of spin coherent states arising from the Fubini-Study metric [19]. The Riemannian curvature K , given by $K = \frac{1}{2S}$ is dependant on the size of the spin system. We see that the “least” classical, $S = 1/2$, state the curvature is maximal at $K = 1$. This reduces smoothly and monotonically with S until in the infinite limit, for the “most” classical state, the curvature is zero. Hence the curvature of the underlying space seems to be related in some way to the classicality.

One very illuminating way to see the difference in the measurement process as we change S or p_A, p_B is to represent the states and the POVM measures on the Riemann sphere using Majorana representation. In this system, a state with spin S is represented by $2S$ points on a Riemann sphere. The position of these points is given by the zeros of a complex function, constructed from the overlap of the state with a non normalised spin coherent state. The overlap between a non normalised spin coherent state $|\tilde{z}\rangle$ and $|n\rangle$, given by

$$\langle \tilde{z} | n \rangle = \binom{2S}{n}^{1/2} z^n \quad (13)$$

The general state $|\psi\rangle = \sum_{n=0}^{2s} a_n |n\rangle$ is described (up to a global phase) by the overlap function in z (also known as the “coherent-state decomposition” [20] or the “amplitude function” [7])

$$\psi(z) = \langle z | \psi \rangle = \sum_{n=0}^{2s} \binom{2s}{n} a_n z^n \quad (14)$$

$$= N \prod_{i=1}^{2s} (z - z_i) \quad (15)$$

where N is simply a normalisation constant.

The zeros of this function describe the state $|\psi\rangle$ entirely, again up to a global phase. To plot these points onto the sphere we view them as stereographic projections from the north pole onto the complex plane going through the equator. Thus a zero on the plane marks the south pole and as the modulus of the root tends to infinity we get a point at the north pole - this happens when $\psi(z)$ is of order less than n , the multiplicity of points at the north pole is equal to the difference between the order of $\psi(z)$ and the dimension n minus one, thus the state $|0\rangle$ is represented by $2S$ points at the north pole. The projection of $z = \frac{e^{i(\pi-\phi)}}{\tan(\theta/2)}$ onto the sphere represents the rotation of a point at the north pole through angle θ around the axis $\hat{n} = (\hat{J}_x \sin(\phi) - \hat{J}_y \cos(\phi))$, i.e. a point with azimuthal and polar angle θ and ϕ respectively. This can also be thought of as representing the rotation $\hat{R}_{\theta, \phi}$ on state $|0\rangle$.

In the $S = 1/2$ case we find the well known Bloch sphere. Then the state $|\psi\rangle = \cos(\theta/2)|0\rangle + e^{i\phi} \sin(\theta/2)|1\rangle$ has an overlap function $\psi(z) = \cos(\theta/2) + e^{i\phi} \sin(\theta/2)$ with one zero at $z = \frac{e^{i(\pi-\phi)}}{\tan(\theta/2)}$ where θ and ϕ are the polar and azimuthal angles respectively, of the 2D Riemann sphere. We also note that the Majorana picture could equally

represent a multiparticle state of $2S$ spin $1/2$ particles in a symmetric superposition. Each point represents one spin $1/2$ particle [21]. Going back to the notion of a beam of spin mentioned in the previous section, each point would then represent a particle in our beam.

We can make a number observations from this definition. Firstly, spin coherent states are represented by $2S$ points all at the same one position on the unit 2-sphere. This is clear since for a spin coherent state $|\alpha\rangle$, the overlap function is $\langle \tilde{z}|\alpha\rangle = \frac{(1+z\bar{\alpha})^{2S}}{(1+|\alpha|^2)^S}$, which has $2S$ zeros at $-1/\bar{\alpha}$. Secondly, any rotation of a state $|\psi\rangle$ rotates the sphere - since when forming the overlap function (equation (14)) we can equally consider the rotation on ψ as a reverse rotation on each of the $|\tilde{z}\rangle$ s, corresponding to the zeros, which is also a rotation of the points around the sphere. Note though, such a rotation can still add a phase that will not be seen on the Majorana sphere. This provides the basis for the next two points.

The modulus of the overlap between any two spin coherent states is given entirely by the angle between their points on the sphere. This is true since any two pairs of spin coherent states with the same angle between them on the Majorana sphere are only a unitary rotation apart (up to phase), since this preserves the overlap up to a phase, any such pairs have equal overlap modulus. Any state with one or more point antipodal to the coherent state is orthogonal. To show this it is sufficient to show it for the case $|\alpha\rangle = |0\rangle$, since we can simply rotate the sphere and maintain any overlap up to a phase. The set of states orthogonal to $|0\rangle$ are given by $|\alpha^\perp\rangle = \sum_{n=1}^{2S} a_n|n\rangle$. The coherent state decomposition thus has $z = 0$ as one of its zeros at least, indeed this can only occur if the state has no components in $|0\rangle$. This gives a Majorana point at the south pole, i.e antipodal.

With this we can begin to look at how the Helstrom discrimination strategy for two spin coherent states can be seen in this representation. The states themselves are shown as two points on the sphere. To represent the projections we show the two resultant states after the measurement takes place, $|e_A\rangle, |e_B\rangle$, corresponding to \hat{E}_A and \hat{E}_B respectively. We can do this because the two states to be distinguished will both collapse onto the same one of two resultant states. This is because any projection we make will be on the two dimensional subspace of the two states, since to project outside this space would not be optimal. Hence, they project onto the same pair of states in this subspace.

The first thing we notice is that for any S , these states give Majorana points that lie on a circle on the surface of the sphere. This is in fact the case for any state that is a superposition of two coherent states. For any complex coefficients a and b , the state $|\psi\rangle = a|0\rangle + b|\beta\rangle$ gives overlap function zeros that lie on a circle of radius $r = \left|\frac{a}{b}\right|^{1/2S} \frac{(1+|\beta|^2)^{1/2}}{|\beta|}$ centred at $-1/\beta$ on the complex plane. The stereographic projection preserves circles and angles [22], hence the Majorana points lie on a circle also (since this is true for the above superposition, it is true for any superposition of 2 coherent states because we can always rotate the pair so one state is $|0\rangle$ and maintain the geometry). Furthermore, the radius and position of these circles relate back to the overlap of the states and their apriori probabilities, though the relationships are complicated and we will talk only about trends qualitatively.

In figure 6 we see the Majorana projection of two spin coherent states, pointed out by two black lines, and the states post projection, pointed out by the light and dark grey lines, that sit on two circles, for $S = 10$. State $|A\rangle = |0\rangle$ sits on the north pole and state $|B\rangle = |-i\rangle$ sits at $(1, 0, 0)$. The light grey lines point to the circle representing projection \hat{E}_A and the dark grey, \hat{E}_B . The apriori probabilities are set at $p_A = p_B = 0.5$.

We can now look at how changing the apriori probabilities and S change the Helstrom measurements we make, found from the minimisation of equation (11). For any fixed spin, as the apriori probability of $|A\rangle$ (or $|B\rangle$) increases, the circle of the corresponding projection \hat{E}_A (\hat{E}_B) closes in around the state until it becomes that state, that is $|e_A\rangle \rightarrow |A\rangle$ ($|e_B\rangle \rightarrow |A_\perp\rangle$) (where $|A_\perp\rangle$ is the state orthogonal to A in the $|A\rangle, |B\rangle$ plane) - as we would expect for minimisation of equation (11). The other circle, for projection \hat{E}_B (\hat{E}_A), widens until it becomes the state orthogonal to $|A\rangle$ ($|B\rangle$) in the $|A\rangle, |B\rangle$ subspace - this is the circle who's width allows one point to sit antipodal to the Majorana point of $|A\rangle$ ($|B\rangle$).

Keeping p_A, p_B fixed and increasing S both circles become larger, as the projected states $|e_A\rangle$ and $|e_B\rangle$ get closer to $|B_\perp\rangle$ and $|A_\perp\rangle$ respectively. This illustrates the reason for decrease in probability of error with S seen in figures (4) and (5). As S increases, the states $|A\rangle$ and $|B\rangle$ become more orthogonal, this allows the projection POVMs to change to be more orthogonal to the anticorresponding states in accordance with the minimisation of equation (11), illustrated by the growth of the circles, where P_e then reduces with S . Therefore, the smooth growth of the projection circles illustrates that within this distinguishability criterion for classicality, spin coherent states approach optical coherent states with the increase of spin. This is in contrast with the previous criterion based on entanglement generation where we see a brief increase of entanglement with spin.

CONCLUSION

In this paper we have extended the analysis of spin coherent states to examine their approach to classicality as the spin, S , goes from the least classical spin $1/2$ to the most classical $S \rightarrow \infty$. We gave an alternative proof that as the spin goes to infinity the spin coherent states become the orthogonal subset of optical coherent states. This is not unique to spin coherent states, indeed there are infinitely many sets of states for which this is true. The spin coherent state does represent an element of these that achieves minimum uncertainty.

We have studied the entanglement generation of spin coherent states for the specific case where it is sent through one arm of a beam splitter and a vacuum through the other. We found the entanglement to be very slow in decreasing as S of the input state increases, and very dependent on amplitude z of the state. We also found that the entanglement went up initially as we increase S for $|z| > 1$. The high dependence on $|z|$, very slow decline to zero and increase of entanglement (thus dip in this measure of classicality) are indicators that this measure may be inadequate as a universal signature of classicality. The value in these results is in the understanding of a beam splitter as an entanglement generator, with respect to which it is also found that the generated entanglement increases with amplitude z , and that for any spin S we can find an amplitude with $|z|$ that gives the maximum entanglement at output. In a sense we have sacrificed the generality of this result as a classicality measure for its simplicity and applicability.

We then looked at distinguishability of two spin coherent states. The probability in error for the Helstrom measure was used as a measure of how distinguishable the states are. As a measure of classicality this is well defined and we see a quick and smooth monotonic increase from $S = 1/2$ to $S \rightarrow \infty$, allowing us to call $S = 1/2$ least classical, with least distinguishability for any two spin coherent states, and the infinite limit $S \rightarrow \infty$ most classical, where all states are fully distinguishable hence in this respect classical.

Noting that the classicality of distinguishability offers a smooth transition from the least $S = 1/2$ to the most classical $S \rightarrow \infty$ spin coherent states we can think of other possible measures. One mentioned earlier in the previous section, is the curvature of the state space according to the Fubini-Study metric, which for the spin coherent state is given by $K = 1/2S$ [19]. Thus, this also gives a smooth transition with S , decreasing from the maximal $K = 1$ for the least classical spin half state, to flatness, $K = 0$, for the limit (most classical). Unlike the classicality of distinguishability, the curvature does not depend on the amplitude z , because the (Riemann) sphere is equally curved at all points. Another measure of classicality might be the distance from the optical coherent states (using any “reasonable” distance measure), which, for example, monotonically decreases to zero in the infinite limit and is smaller for higher z . We reiterate that none of these measures give a common result; they all follow different declines and cannot be said to be equivalent exactly in the transition regime.

Finally we used the Majorana representation to illustrate the Helstrom measurement strategy. The geometry of the states and the Helstrom POVMs is simple and allows us to illustrate easily the changes effecting the probability of error for the measurement. A spin coherent state is simply one point on the sphere and the POVMs are represented by circles of points. The decrease in probability of error with an increase in S is seen by the increase in the diameter of the circles on the sphere representing the measurements. It would be interesting for future work to create a common criteria for ‘classicality measures’ or indicators of states. It seems that one common feature that should be imposed is the monotonicity with S . In addition, we would like the classical states to be the minimum uncertainty states for any pair of canonical (incompatible) observables. One important property we would also need to look is that a classical system should be inefficient at generating entanglement within itself, but on the other hand, should be able to strongly entangle to its environment (this is required for example in decoherence models). It is not at all clear that there exists a single measure that would capture all these desirable properties and this remains a challenging open problem.

Acknowledgements. We would like to thank William Irvine, Manfred Lein and Stefan Scheel for very useful discussions on the subject of this paper and Jens Eisert for critical reading of the proofs involved. This work was sponsored by Engineering and Physical Sciences Research Council, the European Community, the Elsaspa and the Hewlett-Packard company.

-
- [1] M. Gell-Mann and J. Hartle. *Phys. Rev. D*, 47(3345), 1993.
 - [2] R. J. Glauber. *Phys. Rev.*, 131(2766), 1963.
 - [3] Y. Aharonov, D. Falkoff, E. Lerner, and H. Pendelton. A quantum characterization of classical radiation. *Ann. Phys.*, 39(498-512), 1966.
 - [4] J. R. Klauder and B. Skagerstam. Coherent states. *World Scientific, Singapore*, 1985.

- [5] J. R. Klauder. 2001. Contribution to the 7th ICUSSR Conference, June 2001, quant-ph/9601020.
- [6] J. M. Radcliffe. *J. Phys. A*, 4(313-323), 1971.
- [7] F. T. Arrechi, E. Courtens, R. Gilmore, and H. Thomas. *Phys. Rev. A*, 6(2211), 1972.
- [8] M.C. Arnesen, S. Bose, and V. Vedral. *Phys. Rev. Lett.*, 87(017901), 2001.
- [9] N. Gisin. *Phys. Lett. A*, 242(1), 1998.
- [10] R. Loudon. *The Quantum Theory of Light*. Oxford University Press, Oxford, 3 edition, 2000.
- [11] R. A. Campos, B. E. A. Saleh, and M. C. Teich. *Phys. Rev. A*, 40(1371), 1989.
- [12] S. Bose and V. Vedral. *Phys. Rev. A*, 61(040101), 2000.
- [13] J. von Neumann. *Mathematical Foundatins of Quantum Mechanics*. (Eng. translation by R. T. Beyer), Princeton University Press, Princeton, 1955.
- [14] G. Vidal. *J. Mod. Opt.*, 47(355), 2000.
- [15] M. S. Leifer, L. Henderson, and N. Linden. 2002. quant-ph/9601020.
- [16] S. M. Tan, D. F. Walls, and M. J. Collett. *Phys. Rev. Lett.*, 66(252), 1991.
- [17] C. W. Helstrom. *Quantum Detection and Estimation Theory*. Academic Press, New York, 1976.
- [18] C. A. Fuchs. Phd thesis. University of New Mexico, quant-ph/9601020.
- [19] J. P. Provost and G. Vallee. *Commun. Math. Phys.*, 76(289-301), 1980.
- [20] P. Leboeuf. *J. Phys. A: Math. Gen.*, 24(4575), 1991.
- [21] R. Penrose and Rindler. *Spinors and Space Time. Vol.1: Two Spinor Calculus and Relative Fields*. Cambridge University Press, Cambridge, check edition, 1984.
- [22] H. Eves. *A Survey of Geometry*. Allyn and Bacon, Inc. Boston, check edition, 1963.

APPENDIX

Optical coherent states are defined as, [10],

$$\begin{aligned} |\alpha\rangle &= \exp\left(\alpha\hat{a}^\dagger - \frac{1}{2}|\alpha|^2\right) |0\rangle \\ &= \exp\left(-\frac{1}{2}|\alpha|^2\right) \sum_{n=0}^{\infty} \frac{\alpha^n}{(n!)^{1/2}} |n\rangle. \end{aligned} \quad (16)$$

We wish to show that by appropriate substitution the spin coherent state (equation (3)) is equal to a subclass of optical coherent states as S tends to infinity. We know that for any two different spin coherent states, the overlap tends to zero as S tends to infinity, thus the ‘‘amplitude’’ α for the optical case must tend to infinity as S does. We set $\alpha = \sqrt{2S}\bar{z}$. Substituting this into equation (3) we get

$$|z'\rangle = \frac{1}{(1 + \frac{|\alpha|^2}{2S})^S} \sum_{n=0}^{2S} \binom{2S}{n}^{1/2} \left(\frac{\alpha}{2S}\right)^n |n\rangle. \quad (17)$$

To prove the equivalence of the two states in the infinite limit it is sufficient to show that the overlap of an optical coherent state $|\alpha\rangle$ and such a spin coherent state goes to one (i.e. they are the same state).

$$\begin{aligned} \lim_{S \rightarrow \infty} \langle \alpha | z' \rangle &= \lim_{S \rightarrow \infty} \left\{ \exp\left(-\frac{1}{2}|\alpha|^2\right) \frac{1}{(1 + \frac{|\alpha|^2}{2S})^S} \sum_{n=0}^{2S} \left(\frac{2S!}{(2S-n)!(2S)^n}\right)^{1/2} \frac{|\alpha|^{2n}}{n!} \right\} \\ &= 1. \end{aligned} \quad (18)$$

Let us first look at the summation. We wish to prove

Lemma For all $A \in R^+$

$$\lim_{n \rightarrow \infty} \sum_{p=0}^n \left(\frac{n!}{(n-p)!n^p}\right)^{1/2} \frac{A^p}{p!} = \sum_{p=0}^{\infty} \frac{A^p}{p!}. \quad (19)$$

Proof We will use the method of showing that the upper and lower bounds to $\langle \alpha | z' \rangle$ coincide as S tends to infinity. Since each term in the sum is positive, one upper bound of the left hand side of equation (19) can be found by taking the sum to infinity. Thus

$$\lim_{n \rightarrow \infty} \sum_{p=0}^n \left(\frac{n!}{(n-p)!n^p}\right)^{1/2} \frac{A^p}{p!} \leq \lim_{n \rightarrow \infty} \sum_{p=0}^{\infty} \left(\frac{n!}{(n-p)!n^p}\right)^{1/2} \frac{A^p}{p!}$$

$$\leq \sum_{p=0}^{\infty} \frac{A^p}{p!}, \quad (20)$$

where the last line is given by taking the limit inside the sum, which we are allowed to do since each term converges.

We then find a lower bound by taking the sum to some finite m , so

$$\lim_{n \rightarrow \infty} \sum_{p=0}^n \left(\frac{n!}{(n-p)!n^p} \right)^{1/2} \frac{A^p}{p!} \geq \lim_{n \rightarrow \infty} \sum_{p=0}^m \left(\frac{n!}{(n-p)!n^p} \right)^{1/2} \frac{A^p}{p!}. \quad (21)$$

However, taking the infinite limit of m this inequality still holds, since it is true for any finite m and so it is true for any arbitrarily small distance from the limit so the limit can at most be equal. This gives the same upper as lower bound, hence:

$$\begin{aligned} \lim_{n \rightarrow \infty} \sum_{p=0}^n \left(\frac{n!}{(n-p)!n^p} \right)^{1/2} \frac{A^p}{p!} &= \lim_{n \rightarrow \infty} \sum_{p=0}^{\infty} \left(\frac{n!}{(n-p)!n^p} \right)^{1/2} \frac{A^p}{p!} \\ &= \sum_{p=0}^{\infty} \frac{A^p}{p!} \\ &= \exp(A). \end{aligned} \quad (22)$$

Since the normalisation and the summation in equation (18) converge with n , the limit of the product is the product of the limits and thus

$$\begin{aligned} \lim_{S \rightarrow \infty} \langle \alpha | z' \rangle &= \exp(-|\alpha|^2) \exp(|\alpha|^2) \\ &= 1. \end{aligned} \quad (23)$$

Interestingly, this is also true of any state $|\psi\rangle = \sum_{n=0}^{d-1} f(n, d) \frac{A^n}{(n!)^{1/2}} |n\rangle$ such that $f(n, d) > 0, \forall n, d \in \mathbf{N}$ and $f(n, d)$ converges to 1 in n for all p , for example $|z\rangle = \exp(-\frac{1}{2}|z|^2) \sum_{p=0}^{\infty} \frac{z^p}{p!} |p\rangle$. There are infinitely many such functions and therefore there are infinitely many states that will limit to the optical coherent state as stated in section .

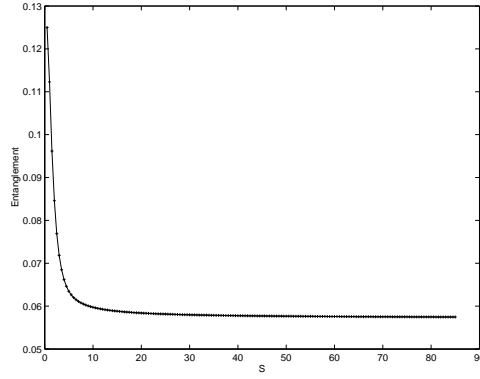


FIG. 1: Linear Entropy of Entanglement against S for $|z|^2 = 1$. As we can see the entanglement reduces quickly at first but then more slowly. Indeed it does not appear straight away to limit to zero (though we know it does).

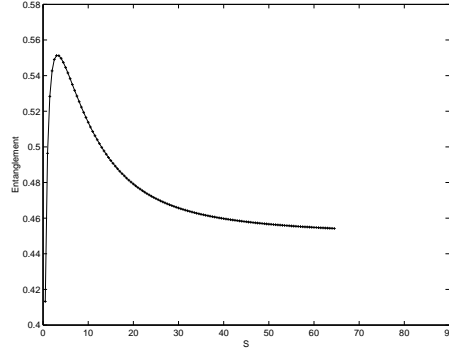


FIG. 2: Linear Entropy of Entanglement against S for $|z|^2 = 10$. Here the Entanglement rises first then tails off after around $S = 40$

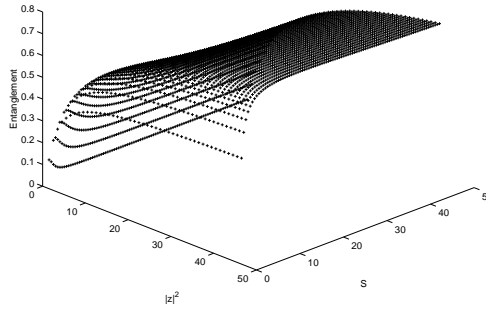


FIG. 3: Linear Entropy of Entanglement against S and $|z|^2$. We see the pattern of a rapid initial peak followed by very slow decrease thereafter for all $|z|^2$, and that an increase in $|z|^2$ increases the entanglement for any S .

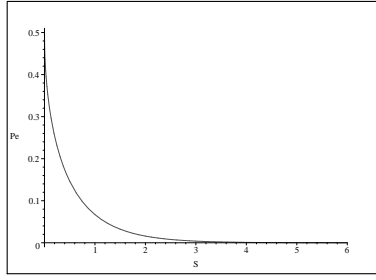


FIG. 4: Probability of Error against S for $p_A = 0.5$ and $\alpha = 0, \beta = 1$. The likelihood of error quickly decreases with S .

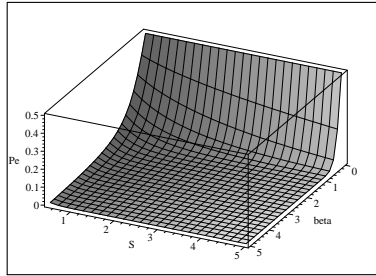


FIG. 5: Probability of Error against S and $\beta(real)$ for $p_A = 0.5$. The likelihood of error quickly decreases with S for all β .

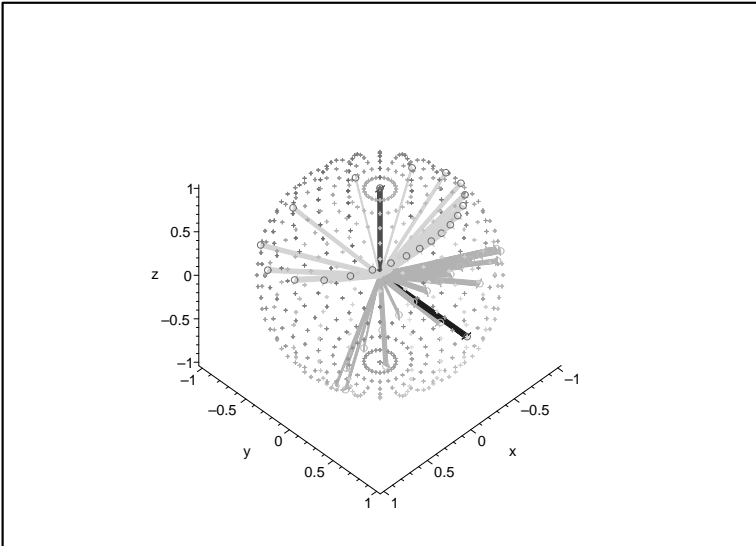


FIG. 6: Majorana projection of two coherent states (pointed by black lines) and the states post projection (circles of points). The light grey lines point to the circle corresponding to the projection \hat{E}_A and the dark grey lines \hat{E}_B .